DOI: 10.21062/mft.2022.066  http://www.journalmt.com

# The Diffusion Coatings for Industrial Tool Application

Marcin Drajewicz[1] (0000-0002-9600-6938), Adrianna Przybylo[2], Jakub Jopek[1], Marek Góral[1]* (0000-0002-7058-510X), Barbara Koscielniak[1](0000-0002-1683-0354), Kamil Ochal[1](0000-0002-0708-2542), Tadeusz Kubaszek[1](0000-0002-7006-4857), Artur Gurak[1], Kamil Dychton (0000-0002-3003-8603) [1], Mateusz Wozniak[2], Pawel Kwasniewski[3](0000-0002-7826-6672), Artur Kawecki[3](0000-0001-8426-449X), Wojciech Gluchowski[4](0000-0001-9356-9674), Marek Lagoda[4](0000-0003-3679-6568)

[1]Research and Development Laboratory for Aerospace Materials, Rzeszow University of Technology, Powstancow Warszawy 12, 35-959 Rzeszow, Poland,

[2]Doctoral School of Engineering and Technical Sciences at the Rzeszow University of Technology, Rzeszow University of Technology, Powstancow Warszawy 12, 35-959 Rzeszow, Poland, Poland

[3]AGH University of Science and Technology, Faculty of Non-Ferrous Metals, Adama Mickiewicza 30, 30-059 Cracow, Poland

[4]Lukasiewicz Research Network - Institute of Non-Ferrous Metals, Józefa Sowińskiego 5, 44-121 Gliwice, Poland
Corresponding author * e-mail: mgoral@prz.edu.pl

**The diffusion boriding process allows increasing the abrasion and corrosion resistance of the majority of steel grades. The aim of this study was to determine the influence of the chemical composition of the substrate of various steel grades on the microstructure of boride coatings produced using two diffusion methods: pack cementation boriding using EKABOR-2 and paste-pack boriding using EKABOR-PASTE on the substrate of tool and structural steels:. The boriding processes were carried out at 1000°C in an argon atmosphere for 4h. Microstructural investigations of the obtained coatings indicate that a high content of alloying elements increasing the FeB (Cr, Mo, W) phase, results in the formation of an external, continuous layer of FeB borides. It was found that with increasing alloying element and carbon concentration, the total thickness of the boride coatings decreases. In particular, chromium content below about 1%, with a carbon content below about 0.4%, significantly limits or prevents the formation of the FeB phase. Increasing the content of alloying elements and carbon, results in a change in the morphology of the iron borides.**

**Keywords:** boride coatings, hard coatings, pack boriding, wear, corrosion

## 1 Introduction

At the end of the 19th century, it was noticed that an increase in the hardness and wear resistance of steel components was possible due to the diffusion of boron atoms deep into their surface layer [1]. Significant improvements in corrosion resistance [2-8] and heat resistance [9] of many steels subjected to diffusion boriding have also been demonstrated. Due to the simplicity and low cost of the method, and most of all, the possibility of significant improvement of functional properties of metallic materials, iron alloys [10-12], nickel [13,14], titanium [15,16] and cast irons [17] have been subjected to boriding, usually at 850 - 1000oC, for 1 - 10 h [18].

The diffusion boriding process can be carried out in solid, liquid or gaseous media, under glow discharge conditions, or by boron ion implantation. Among the many available boriding methods, pack boriding has found the widest practical application, due to the lack of need to use expensive and complicated apparatus and the possibility of easily changing the chemical composition of the boriding mixture [12,19]. It consists of several basic substances: a boron-bearing substance, an activator and filler. The type and content of the boron-bearing substance, which is usually B4C, B2O3, or amorphous boron, determine the saturation capacity of the powder. The presence of an activator (e.g. NaF, NaCl, KBF4, Na2B4O7) in an amount of a few wt.% increases the intensity of transport of boron atoms from the saturating medium through the gas phase to the substrate surface of the workpiece, significantly shortening the processing time. The last component of the mixture is an inert filler (e.g. Al2O3, MgO, kaolin, SiC), which prevents sintering of the powder during the process and reduces the boron potential, counteracting the formation of a brittle FeB phase.

In the diffusion boriding process, the previously cleaned components are placed in a heat-resistant steel container, backfilled with the powder mixture and sealed with low-melting glass. The container is then placed in an electric resistance furnace at atmospheric pressure, heated to 850 - 1100oC and held for 2-24 h [10,12,18]. The mechanism of the boriding process starts with the heat-activated diffusion of boron atoms

and their adsorption on the surface of the substrate material. Then the boron atoms build into the crystal lattice, diffuse deep into the element to form borides. In order to determine the kinetics of the boriding process, experimental processes are carried out for different steels constituting the substrate material [20-24]. Numerical methods for modelling the kinetics of the boriding process are also being developed [25-30].

The study [31] describes the mechanism of formation of boride layers on 34CrAlMo5-10 steel substrate. Depending on the boriding potential of the mixture used [32], the chemical composition of the substrate and the process parameters, single or two-phase coatings were formed. Below the layer composed of FeB and Fe2B iron borides, there was a diffusion zone - a solid solution of boron in iron. Within this zone, as a result of boron and carbon supersaturation, carbide borides of iron or alloying elements may form [10,19]. Due to the high brittleness of FeB borides, a two-phase microstructure (FeB+Fe2B) is undesirable. Additionally FeB borides are characterized by a different value of the thermal expansion coefficient compared to Fe2B. This results in the formation of significant tensile stresses in the two-phase layers during cooling after the boriding process, which are the cause of the appearance of cracks at the boride boundaries [10,11,18].

By modifying the carbon and alloying element content, it is possible to influence the thickness and morphology of boride coating. The optimum coatings thickness for low-carbon and low-alloy steels is 50 - 250 um, while for high-alloy steels it is in the range of 25 - 76 um [11]. In low-carbon and low-alloy steels, the borides formed have a needle-like structure [28] providing exceptional adhesion to the substrate [33]. Due to the lower brittleness and favourable compressive stress state, a coating consisting exclusively of Fe2B borides is desirable. In high-alloy steels, alloying elements such as Cr, Ni, Mo, W, V concentrate at the vertices of the resulting boride columns, causing a reduction in the diffusion flux of boron atoms in these zones. This results in inhibition of vertex growth, leading to formation of a flat boride/substrate interfacial boundary. Increasing the Cr content to about 6% results in the complete disappearance of the needle-like structure and an increase in the proportion of the FeB phase [10,11]. This was confirmed, among others, in the ref. [34], where the boriding of AISI 310 stainless steel containing 25% Cr and 19.5% Ni resulted in a flat front of boride coatings composed of iron, nickel and chromium borides. The Si and Al present in the steel reduce the boride growth kinetics and are pushed out in front of the boride front, forming a band of low hardness ferrite [10]. A recent study [35] suggests that Mn increases the growth kinetics of boride layers and produces a needle-like morphology of them. High carbon content in steels is also the reason for obtaining a smoothed boride front. The reason for this is the lack of solubility of carbon in FeB and Fe2B, which forces its diffusion into the steel, leading to an increase in its concentration in front of the growing boride front. This, in turn, results in a slower diffusion of boron, causing a "smoothing" of the boride/substrate interfacial boundary and a decrease in the thickness of the films obtained [10,11,18]. A flat front of FeB and Fe2B borides was obtained by boriding AISI M2 high speed steel [20,27], AISI D3 tool steel [36] and high-alloy cold work steel containing 0.9% C, 7.8% Cr, 2.5% Mo, 0.5% Mn, 0.5% V [9].

The resulting boride coatings enable the improvement of many performance properties of the steel substrate. Apart from the obvious increase in the hardness of the surface layer, powder-pack boriding allows for a significant improvement in abrasive wear resistance: 41-fold AISI 316L stainless steel [37,38], 7-fold AISI 310 heat-resistant austenitic steel [34], 13-fold AISI H13 and AISI D2 tool steels [39], 5-fold AISI H10 tool steel [40] and C35 steel [7], 4-fold D6 tool steel [41], and 7-fold Hardox 450 and HiTuf steel [42]. Significant improvements can also be achieved in corrosion resistance: 17-fold tool steel in 4% HCl solution [8] and 4 to 6-fold C35 steel in 5% H2SO4, HCl, HNO3, NaCl, NaOH solutions [3]. In addition, pack boriding of AISI 316L SS steel allowed a 2-fold increase in its resistance to high-temperature oxidation (24h/1000oC). Studies have also been carried out on the fracture resistance of boride coatings [43] and their adhesion to the substrate [44].

Despite a number of advantages resulting from the application of the boriding process to the treatment of steel machine parts, nitriding and carburising are still much more frequently used in industrial practice. In the available publications, there is no data on the boriding of many steel grades with different alloying element contents. The influence of alloying elements on the microstructure of borated steels is extremely important and allows optimisation of the process parameters in order to obtain coatings with the desired properties. Therefore, the aim of this study was to determine the influence of the chemical composition of the substrate of various steel grades on the microstructure of boride coatings produced using two diffusion boriding methods: pack boriding using EKABOR-2 and paste-pack boriding using EKABOR-PASTE on the substrate of tool and structural steels.

## 2 Experimental

The substrate material used in the study was supplied in the form of bars with a diameter of ϕ30 or ϕ35 mm, (depending on availability) from which 30 mm high samples were cut. The processes were carried out on 13 selected steel grades, which are listed in Table 1. The next stage was grinding using an ATM-M SAPHIR 330 grinder-polisher with water-resistant abrasive papers of 80 to 500 mesh. The samples prepared in this way were subjected to diffusion boriding

The diffusion boriding processes were carried out using EKABOR-2 powder with the composition (wt. %): 90%, SiC, 5% $B_4C$, 5% $KBF_4$ and EKABOR-PASTE paste of identical composition.
The process was carried out using a Bernex BPX Pro 325S at 1000°C for 4 hours in an argon atmosphere. After the boriding process metallographic samples were prepared. The microstructure was studied using a Phenom XL scanning electron microscope (SEM) equipped with an EDS spectrometer - Energy Dispersive X-ray Spectroscopy. The obtained boride layers were assigned to different groups according to the classification proposed by Voroshnin and Lyakhovich [19] and previously conducted XRD analysis of similar coatings [58].

## 3 Results

### 3.1 The Results of microstructure investigation of boride coatings on tool steel substrates

On the substrate of 145Cr6 (NC6) tool steel, after pack boriding in EKABOR-2 (Fig. 1b), a coating was formed consisting of two zones: an outer, continuous FeB (18 um) and inner, continuous $Fe_2B$ (67 um). The formation of FeB is due to the presence of Mn and Cr in the steel, which increase its amount [19]. According to previous XRD analysis [58] as well as the classification adopted, the structure obtained was assigned to structure model no. I [19]. However, after paste-pack boriding in EKABOR-PASTE (Fig. 1a), only a continuous layer of $Fe_2B$ borides (85 um) was formed, which allows it to be classified as structure no. II. The low content of alloying elements makes the morphology of the formed borides needle-like in both cases.

Pack boriding with EKABOR-2 of X165CrV12 steel (NC10) resulted in the formation of a two-zone coating (Fig. 2b): an outer, continuous FeB (12 um) and inner, continuous $Fe_2B$ (33 um). The high Cr content in the steel substrate favors the formation of FeB borides. According to XRD analysis [58] and literature data [19], this structure was classified as no. I. Boriding in EKABOR-PASTE (Fig. 2a) resulted in a single-zone continuous $Fe_2B$ (50 um) coating, which corresponds to model no. II. In both cases the resulting coatings were blunted and branched, which is a consequence of the high Cr content in the substrate [19].

***Tab. 1*** *Chemical composition of substrate materials - tested steel grades according to standards: PN-EN 10088-1, PN-EN 10085, PN-EN 10084:2008, PN-EN 10083-3, PN-89/H-84030/02, PN-EN ISO 4957, PN-86/H-85023*

| 145Cr6 (NC6) | | | | | | | | | | | |
|---|---|---|---|---|---|---|---|---|---|---|---|
| C: | Mn: | Si: | P: | S: | Cr: | Mo: | Ni: | V: | Co: | Cu: | W: |
| 1.30-1.45 | 1.40-1.70 | 0.15-0.40 | <0.03 | <0.03 | 1.30-1.65 | - | - | 0.10-0.25 | - | - | - |
| X165CrV12 (NC10) | | | | | | | | | | | |
| C: | Mn: | Si: | P: | S: | Cr: | Mo: | Ni: | V: | Co: | Cu: | W: |
| 1.50-1.80 | 0.15-0.45 | 0.15-0.40 | <0.03 | <0.03 | 11.0-13.0 | - | - | - | - | - | - |
| X153CrMoV12 (NC11LV) | | | | | | | | | | | |
| C: | Mn: | Si: | P: | S: | Cr: | Mo: | Ni: | V: | Co: | Cu: | W: |
| 1.45- 1.60 | 0.20-0.60 | 0.10-0.60 | <0.03 | <0.02 | 11.0-13.0 | 0.70-1.00 | | 0.70-1.00 | - | - | - |
| 90MnCrV8 (NMV) | | | | | | | | | | | |
| C: | Mn: | Si: | P: | S: | Cr: | Mo: | Ni: | V: | Co: | Cu: | W: |
| 0.85-0.95 | 1.80-2.20 | 0.10-0.40 | <0.03 | <0.03 | 0.20-0.50 | - | - | 0.05-0.20 | - | - | - |
| 60WCrV8 (NZ3) | | | | | | | | | | | |
| C: | Mn: | Si: | P: | S: | Cr: | Mo: | Ni: | V: | Co: | Cu: | W: |
| 0.55-0.65 | 0.15-0.45 | 0.70-1.00 | <0.03 | <0.02 | 0.90-1.20 | - | - | 0.10-0.20 | - | - | 1.70-2.20 |
| X37CrMoV5-1 (WCL) | | | | | | | | | | | |
| C: | Mn: | Si: | P: | S: | Cr: | Mo: | Ni: | V: | Co: | Cu: | W: |
| 0.33-0.41 | 0.25-0.50 | 0.8-1.2 | <0.03 | <0.02 | 4.80-5.50 | 1.10-1.50 | - | 0.30-0.50 | - | - | - |
| HS6-5-2 (SW7M) | | | | | | | | | | | |
| C: | Mn: | Si: | P: | S: | Cr: | Mo: | Ni: | V: | Co: | Cu: | W: |
| 0.80-0.88 | <0.4 | <0.45 | <0.03 | <0.03 | 3.80-4.50 | 4.70-5.20 | - | 1.70-2.10 | - | - | 5.90-6.70 |
| 18NiCrMo7-6 (17HNM) | | | | | | | | | | | |
| C: | Mn: | Si: | P: | S: | Cr: | Mo: | Ni: | V: | Co: | Cu: | W: |
| 0.14-0.19 | 0.40-0.70 | 0.17-0.37 | <0.035 | <0.035 | 1.50-1.80 | 0.25-0.35 | 1.40-1.70 | - | - | - | - |
| S355 (18G2A) | | | | | | | | | | | |
| C: | Mn: | Si: | P: | S: | Cr: | Mo: | Ni: | V: | Co: | Cu: | W: |
| <0.20 | <1.50 | 0.20-0.50 | <0.035 | <0.035 | <0.30 | - | <0.30 | - | - | <0.30 | - |
| 16MnCr5 (16HG) | | | | | | | | | | | |
| C: | Mn: | Si: | P: | S: | Cr: | Mo: | Ni: | V: | Co: | Cu: | W: |
| 0.14-0.19 | 1.00-1.30 | <0.40 | 0.025 | <0.035 | 0.90-1.20 | - | - | - | - | - | - |
| 41CrAlMo7-10 (38HMJ) | | | | | | | | | | | |
| C: | Mn: | Si: | P: | S: | Cr: | Mo: | Ni: | V: | Al.: | Cu: | W: |
| 0.38-0.45 | 0.40-0.70 | <0.4 | <0.025 | 0.035 | 1.50-1.80 | 1.20-0.35 | - | - | 1.80-1.20 | - | - |
| X12Cr13 (1H13) | | | | | | | | | | | |
| C: | Mn: | Si: | P: | S: | Cr: | Mo: | Ni: | V: | Co: | Cu: | W: |
| 0.08- 0.15 | <1.5 | <1 | <0.04 | <0.015 | 11.5- 13.5 | - | <0.75 | - | - | - | - |
| 34CrNiMo6 (34HNM) | | | | | | | | | | | |
| C: | Mn: | Si: | P: | S: | Cr: | Mo: | Ni: | V: | Co: | Cu: | W: |
| 0.30-0.38 | 0.50-0.80 | <0.40 | <0.025 | <0.035 | 1.30-1.70 | 0.15-0.30 | 1.30-1.70 | - | - | - | - |

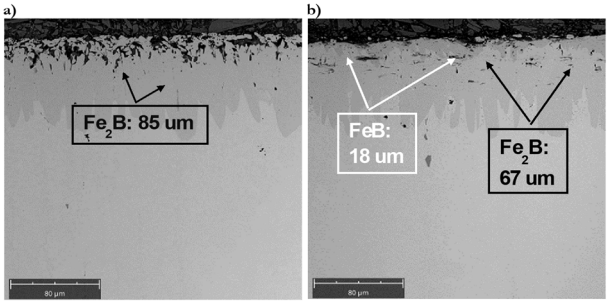


***Fig. 1*** *Cross-section of boride coating formed on 145Cr6 (NC6) steel substrate. Paste-pack boriding in EKABOR-PASTE (a) and pack boriding in EKABOR-2 (b): 1000°C, 4 hours*

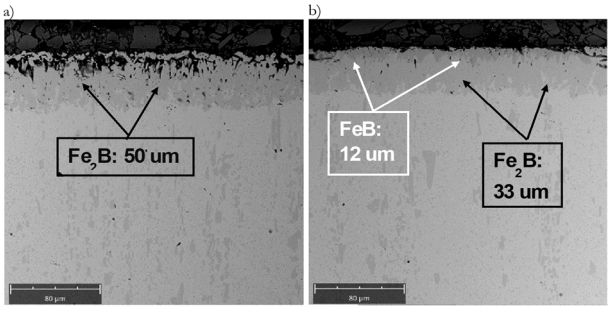


***Fig. 2*** *Cross-section of boride coating produced on X165CrV12 (NC10) steel substrate. Paste-pack boriding in EKABOR-PASTE (a) and pack boriding in EKABOR-2 (b): 1000°C, 4 hours*

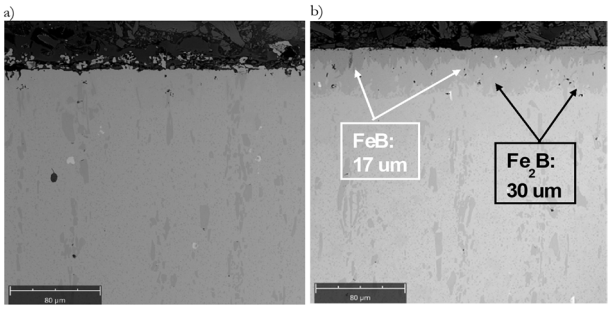


***Fig. 3*** *Cross-section of the boride coating produced on the substrate of X153CrMoV12 (NC11LV) steel. Paste-pack boriding in EKABOR-PASTE (a) and pack boriding in EKABOR-2 (b): 1000°C, 4 hours*

After pack boriding of X153CrMoV12 (NC11LV) steel, an outer continuous FeB boride layer (17 um) and an inner continuous $Fe_2B$ layer (30 um) were obtained (Fig. 3b) [58]. This steel contains Cr, V and Mo, which increases the amount of FeB phase very strongly, hence the greater thickness compared to NC10 steel. The resulting coatings were blunted and branched, which is a consequence of the high alloying element content [19, 58]. Such a structure was assigned to model No. I [19]. Boriding this steel in a paste did not produce a boride coating (Fig. 3a). Oliveira et al. [45] carried out a boriding process for similar AISI D2 steel using a borax bath with 10 wt.% Al. Al (1000°C/4h), which resulted in an outer zone of FeB and an inner zone of $Fe_2B$, with a total thickness of 90 um and a typical needle-like shape of the resulting phases. In comparison, pack boriding in EKABOR-3 of this steel (at 900°C for 2-8h), resulted in the formation of boride coatings with thicknesses ranging from 24 to 40 um [46].

On the substrate of 90MnCrV8 (NMV) steel, a discontinuous outer layer of FeB borides (4 um) and a continuous inner layer of $Fe_2B$ borides (77 um) were formed by pack boriding (Fig. 4b). This phase composition [58] and structure were classified as model no. XI [19]. Paste boriding (Fig. 4a) resulted in a continuous $Fe_2B$ boride layer (92 um), allowing this structure to be assigned to model no. II [19]. In both cases the boride layer had a needle-like structure, which may be due to the low content of alloying elements (including about 2% Mn) in the steel.

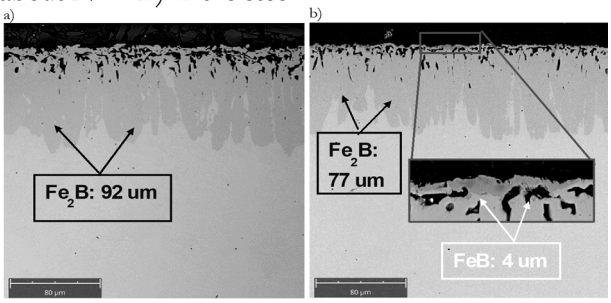


***Fig. 4*** *Cross-section of a boride coating produced on a 90MnCrV8 (NMV) steel substrate. Paste-pack boriding in EKABOR-PASTE (a) and pack boriding in EKABOR-2 (b): 1000°C, 4 hours*

Pack boriding of 60WCrV8 steel (NZ3) led to the formation of a two-zone boride coating (based on XRD ref. [58]), consisting of a discontinuous FeB (7 um) boride layer and a continuous $Fe_2B$ (62 um) layer, so this structure (Fig. 5b) was assigned to model no. XI [19]. After paste boriding, a discontinuous, single-zone $Fe_2B$ (54 um) layer was formed (Fig. 5a), which allowed this structure to be assigned to model no. IX [19]. In both cases the borides have a needle-like shape. Furthermore, a large number of bright precipitates were observed between and under the needles of the $Fe_2B$ borides. According to [19], this may be silicon ferrite, formed due to the expulsion of silicon in front of the front of the growing borides.

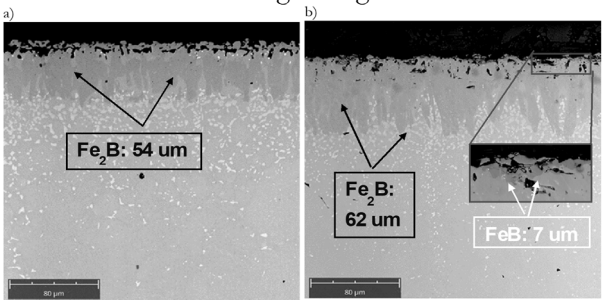


***Fig. 5*** *Cross-section of a boride coating produced on a substrate of 60WCrV8 (NZ3) steel. Paste-pack boriding in EKABOR-PASTE (a) and pack boriding in EKABOR-2 (b): 1000°C, 4 hours*

On the substrate of X37CrMoV5-1 (WCL) steel, two zones were formed in coating produced by pack boriding process (Fig. 6b): an outer continuous FeB layer (25 um) and an inner continuous $Fe_2B$ layer (47 um). This structure is due to the high content of Cr and Mo, which strongly increase the amount of FeB phase [based on XRD ref. 58]. This structure was classified as model no. I [19]. In contrast, paste boriding resulted in the formation of an exclusively continuous $Fe_2B$ boride zone (99 um) and was therefore assigned to model no. II [19]. The both boride coatings formed were characterised by a needle-like structure. A small number of bright precipitates were observed under the $Fe_2B$ layer, which may be compounds of elements pushed out in front of the front of the growing borides [19]. In a study [47], the steel was pack-borided in EKABOR-II powder at 950°C for 5h. A coating of FeB (15 um) + $Fe_2B$ (43 um) borides with a needle-like morphology was formed [58]. A powder mixture was also used consisting of 90 wt.%. $B_4C$ + 10 wt.%. $NaBF_4$, obtaining for 1000°C and 4h process, a FeB (outer) + $Fe_2B$ (inner) boride layer with a total thickness of 110 um [48].

In the case of HS6-5-2 steel (SW7M), pack boriding (Fig. 7b), led to the formation of boride layers: continuous FeB (13 um) and continuous $Fe_2B$ (29 um) (based on XRD in ref. [58]). The continuous and compact FeB layer is due to the high content of alloying elements increasing the amount of the FeB phase (Cr, Mo, W). However, their high content (ca. 18 wt.%), together with ca. 0.84 wt.%. C, resulted in a low total thickness of the produced boride layers [19]. This microstructure was assigned to model no. I. Paste boriding (Fig. 7a) resulted in a single-zone continuous $Fe_2B$ boride lcoating (53 um)-model II. In ref. [20], similar AISI M2 steel was pack borided in EKABOR-I at 850-1050°C for 2-8h. The results of microscopic observations and XRD analysis confirmed the presence of FeB and $Fe_2B$ borides with a flat front, the thickness of which increased parabolically with increasing time and temperature of the boriding process (3-141 um). In another publication [4], the steel in question was subjected to pack boriding in EKABOR-II powder at 950°C for 6h, obtaining a coating 55 um thick consisting of FeB and $Fe_2B$ borides, among others. The authors of the article [49] demonstrated the presence of a biphasic boride zone: FeB + $Fe_2B$ with a needle-like morphology, formed by paste boriding AISI M2 steel in Durborid© at 900- 1000°C for 1-7h. The thickness of the coatings increased with increasing process time and temperature from 10 to 66 um. A contour plot have FeB and $Fe_2B$ boride thickness as a function of powder-pack boriding time and temperature in AISI M2 steel was also proposed [27]. According to the diagram, when boriding at 1000°C for 4h, the estimated layers thicknesses are as follows: 28 um $Fe_2B$ and 17 um FeB, which is in agreement with the obtained experimental results.

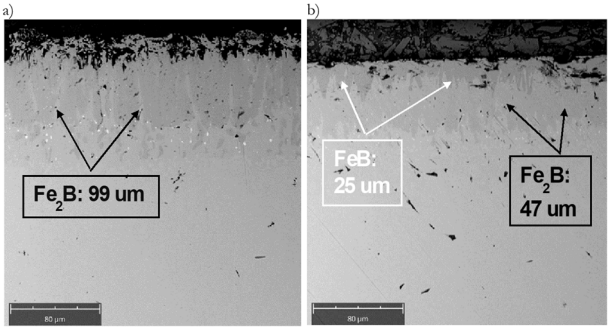


***Fig. 6*** *Cross-section of boride coating produced on X37CrMoV5-1 (WCL) steel substrate. Paste-pack boriding in EKABOR-PASTE (a) and pack boriding in EKABOR-2 (b): 1000oC, 4 hours*

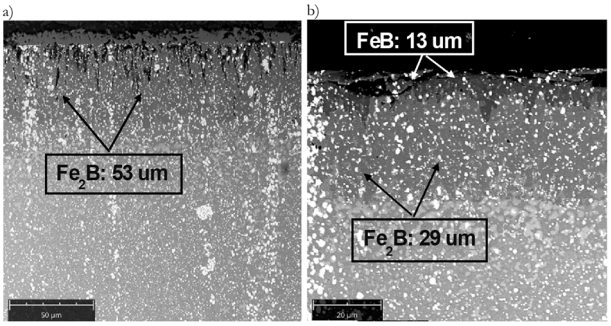


***Fig. 7*** *Cross-section of boride coating produced on HS 6-5-2 (SW7M) steel substrate. Paste-pack boriding in EKABOR-PASTE (a) and pack boriding in EKABOR-2 (b): 1000°C, 4 hours*

### 3.2 Microstructure of boride coatings on the substrate of structural and stainless steels

Both pack boriding of 18NiCrMo7-6 (17HNM) steel (Fig. 8b) and in paste (Fig. 8b) resulted in the formation of a single-zone continuous $Fe_2B$ layer (83 um and 141 um thick, respectively), making these structures classified as model no. II [19, 58]. The borides formed have a branched shape.

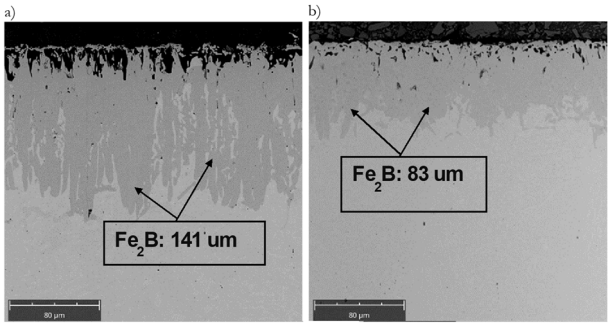


***Fig. 8*** *Cross-section of a boride lcoating produced on a substrate of 18NiCrMo7-6 (17HNM) steel. Paste-pack boriding in EKABOR-PASTE (a) and pack boriding in EKABOR-2 (b): 1000°C, 4 hours*

Powder-pack boriding of S355 steel (18G2A) resulted in an outer, discontinuous FeB layer (5 um) and an inner, continuous $Fe_2B$ layer (Fig. 9b) with a slightly branched shape (88 um), which allowed this phase composition [58] and structure to be classified as model No. XI [19]. In contrast, the effect of Paste-pack boriding (Fig. 9a) was the presence of only a discontinuous $Fe_2B$ boride layer (73 um) with a needle-like morphology, so this structure was assigned to model no. IX [19].

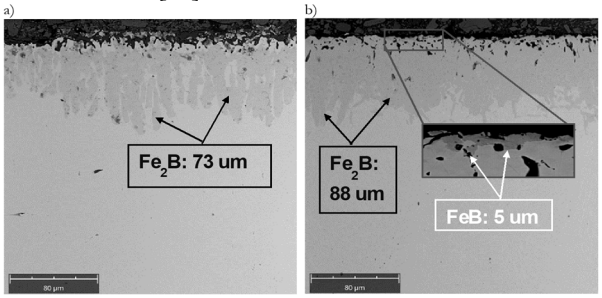


***Fig. 9*** *Cross-section of a boride coating produced on a substrate of S355 steel (18G2A). Paste-pack boriding in EKABOR-PASTE (a) and pack boriding in EKABOR-2 (b): 1000°C, 4 hours*

On the substrate of 16MnCr5 (16HG) steel, based on XRD phase analysis [58] and microscopic examination two-zone discontinuous FeB layer (4 um) and a continuous $Fe_2B$ layer (78 um) was formed by pack boriding (Fig. 10b), which is consistent with model no. XI of the classification used [19]. The resulting $Fe_2B$ borides have, characteristic of low carbon steel, a needle-like shape [19], which has been confirmed in the literature [44, 50]. Paste boriding (Fig. 10a) resulted in the formation of a discontinuous layer of $Fe_2B$ borides in the form of irregularly shaped precipitates (53 um), allowing this structure to be classified as consistent with model no. IX [19].

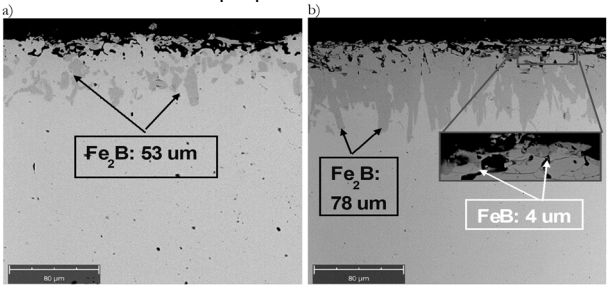


***Fig. 10*** *Cross-section of a boride coating produced on a substrate of 16MnCr5 (16HG) steel. Paste-pack boriding in EKABOR-PASTE (a) and pack boriding in EKABOR-2 (b): 1000oC, 4 hours*

The pack boriding of 41CrAlMo7-10 (38HMJ) steel (Fig. 11b) resulted in two layers: an outer, discontinuous FeB (6 um) and an inner, continuous $Fe_2B$ (86 um), with a needle-like shape [58]. It was classified as structure no. XI [19]. The results obtained are in agreement with those reported in [31], where 34CrAlMo5-10 steel was subjected to Boropack™ pack boriding (1050°C/4h), identifying by XRD [58] analysis small separations of the FeB phase in some regions on the sample surface. Boropack™ pack boriding (Fig. 11a) resulted in the formation of an exclusively discontinuous layer of columnar $Fe_2B$ boride precipitates (99 um) perpendicular to the surface, which is characteristic of the No. IX structure model [19].

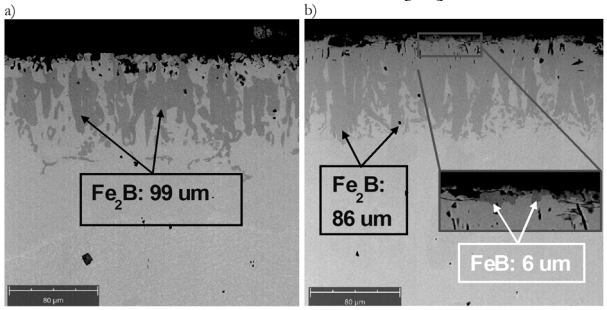


***Fig. 11*** *Cross-section of a boride coating produced on a substrate of 41CrAlMo7-10 (38HMJ) steel. Paste-pack boriding in EKABOR-PASTE (a) and pack boriding in EKABOR-2 (b): 1000oC, 4 hours*

Pack boriding in X12Cr13 (1H13) steel led to the formation of a two-zone boride coating (Fig. 12b) consisting of (based on XRD ref. [58]): an outer, continuous FeB layer (19 um) in the shape of thin needles, and an inner, continuous $Fe_2B$ layer (41 um), below which there were separations of this phase, with a near globular shape. This structure of the microstructure allows it to be classified as model no. I. Similar results were obtained by pack boriding in EKABOR-I on AISI 420 steel (900°C/2-6h). Dense coatings composed of FeB + $Fe_2B$ borides with a total thickness of 27 - 48 um were obtained [51]. On the other hand, in the study of the ref. [52], where pack boriding in EKABOR-II powder was applied to AISI 420 steel (950°C/5h), a layer composed of FeB and $Fe_2B$ borides with a total thickness of 51 um and a flat front was also found. The boriding process in the powder resulted in the formation of a single, continuous $Fe_2B$ layer (89 um) with an irregular shape, below which there were separations of this phase with a near globular shape, therefore this structure was classified as model no. II [19].

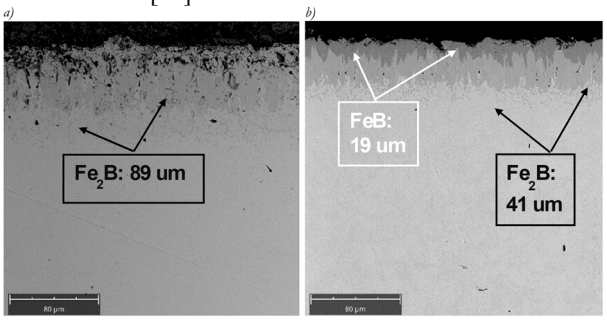


***Fig. 12*** *Cross-section of boride coating produced on X12Cr13 (1H13) steel substrate. Paste-pack boriding in EKABOR-PASTE (a) and pack boriding in EKABOR-2 (b): 1000°C, 4 hours*

In the case of 34CrNiMo6 steel (34HNM), both pack boriding (Fig. 13b) and paste boriding (Fig. 13a) produced continuous $Fe_2B$ layers (XRD – ref. [58]) (77 um and 134 um thick, respectively), so these structures were classified as model No. II [19]. The resulting layers had a distinctly needle-like morphology. Other results were obtained in paper [53], where pack boriding in EKABOR-II powder of this steel, at 850-950°C for 6h, resulted in a characteristic coating composed of FeB borides (outer) and $Fe_2B$ (inner) with thicknesses ranging from 22 to 145 um. Also in ref. [54], boriding in EKABOR-II (950°C/6h), resulted in a two-phase, needle-like coating of FeB + $Fe_2B$ borides with a total thickness of 60 um.

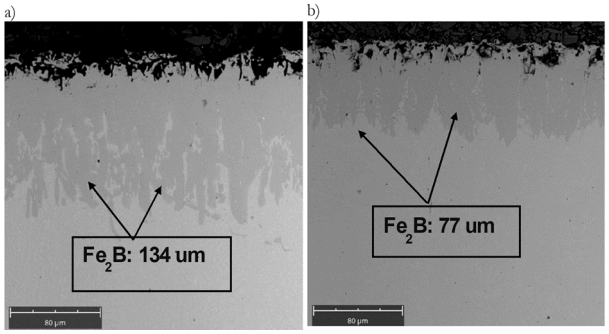


***Fig. 13*** *Cross-section of a boride coating produced on a substrate of 34CrNiMo6 (34HNM) steel. Paste-pack boriding in EKABOR-PASTE (a) and pack boriding in EKABOR-2 (b): 1000°C, 4 hours*

## 4 Discussion

Table 2 shows the classification of the boride coatings obtained on the substrates of the studied steel grades. On the other hand, Figs. 14 - 15 shows the measured thicknesses of boride layers obtained by pack boriding and paste boriding. A clear effect of the content of alloying elements which favour the formation of the FeB phase (i.e. Cr, Mo, W) on the thickness and composition of the boride layers formed was observed. As their content in the steel increased, the thickness of the FeB borides increased, but the total thickness of the layers decreased, which was observed when comparing steels with similar carbon contents (SW7M and NMV) but with significantly different alloying element contents. These results are consistent with literature data [11,19]. Similar observations were made for NC11LV and NC10 steels (about 12 wt.% Cr each), for which boride layers were obtained with a total thickness lower than that produced on NC6 steel (about 1.5 wt.% Cr) by about 40 um. Due to the lower chromium content in the NC6 steel, FeB borides with non-uniform thicknesses were obtained. Furthermore, the $Fe_2B$ needles were thicker and more blunted, compared to those produced on NC10 and NC11LV steels. Increasing the carbon content of the steel results in a decrease in the total thickness of the boride coating and a "smoothing" of the boride/substrate interfacial boundary [10,11,18]. Comparing the obtained microstructures of boride coatings on substrates of steels with similar alloying element contents, i.e. 1H13 and NC10, one can clearly see the effect of carbon on the morphology and thickness of the boride layers formed. Sharp, thin boride needles with a total thickness of 60 um were obtained on the substrate of corrosion-resistant steel 1H13 (ca. 0.1 wt.% C). On the other hand, on the substrate of cold work tool steel NC10 (approx. 1.65 wt. %.C), the resulting borides were blunted and branched, with a total thickness of 45 um. A high carbon content (0.9 wt.%), with a low content of elements promoting the formation of the FeB phase, resulted in a discontinuous layer of FeB borides (e.g. NMV steel). Also, too low a carbon content, combined with an insufficient content of suitable alloying elements, prevented the formation of a continuous FeB phase in the surface layer of the borated steel (e.g. steel NZ3). In order to obtain a continuous, two-zone boride coating, consisting of an outer FeB phase layer and an inner Fe2B layer, an appropriate combination of carbon and alloying elements is required. Steels meeting these requirements, for which the results obtained are in agreement with the available literature, are: SW7M [4,20,27,49], NC11LV [45,46], NC10, 1H13 [51,52], WCL [47,48], NC6. In the case of the boriding of the other steels, comparable thicknesses of boride coatings consisting of $Fe_2B$ phase only (17HNM, 34HNM) or $Fe_2B$ phase and FeB islands (16HG, 38HMJ, 18G2A) were obtained. Due to the insufficient content of alloying elements conducive to the formation of a continuous FeB layer and too low carbon content, it was not possible to obtain on these steels the microstructure characterized as model no. I according to Voroshnin and Lyakhovich [19]. However, $Fe_2B$ boride layers with thicknesses much greater than those formed on tool steels and corrosion-resistant steels were obtained.

In the case of boriding steels in EKABOR-PASTE, a clear effect of carbon and alloying elements on the thickness and morphology of the boride coatings formed was also observed (Fig.15). The coatings formed on steels with a low content of alloying elements and carbon (17HNM and 34HNM) were characterised by a clearly needle-like body and the greatest thickness, equal to about 135 um. In contrast, boride layers with a flat front and a thickness not exceeding 90 um were formed on the substrate of NC10, SW7M and 1H13 steels. This is a result of both the high alloying element and carbon content of these steels. No continuous $Fe_2B$ boride layer was formed on some steels (NZ3, S355, 16HG, 38HMJ), while no boride phases were observed on NC11LV. This is probably due to the application of an inadequate amount of paste, or its uneven distribution prior to the diffusion

boriding process. A higher porosity of the near-surface zone of the boride coatings produced by the paste boriding process was also observed.

The results obtained indicate that the boriding process can be an alternative to the vacuum carburising [55, 56] and plasma nitriding [57] processes studied previously. At a further stage, it will be necessary to investigate the effect of boriding time on the microstructure and phase composition of boride coatings on the analysed steel grades [58-60]. As an alternative the duplex coating with plasma nitriding and PVD coatind deposition might be also considered [61].

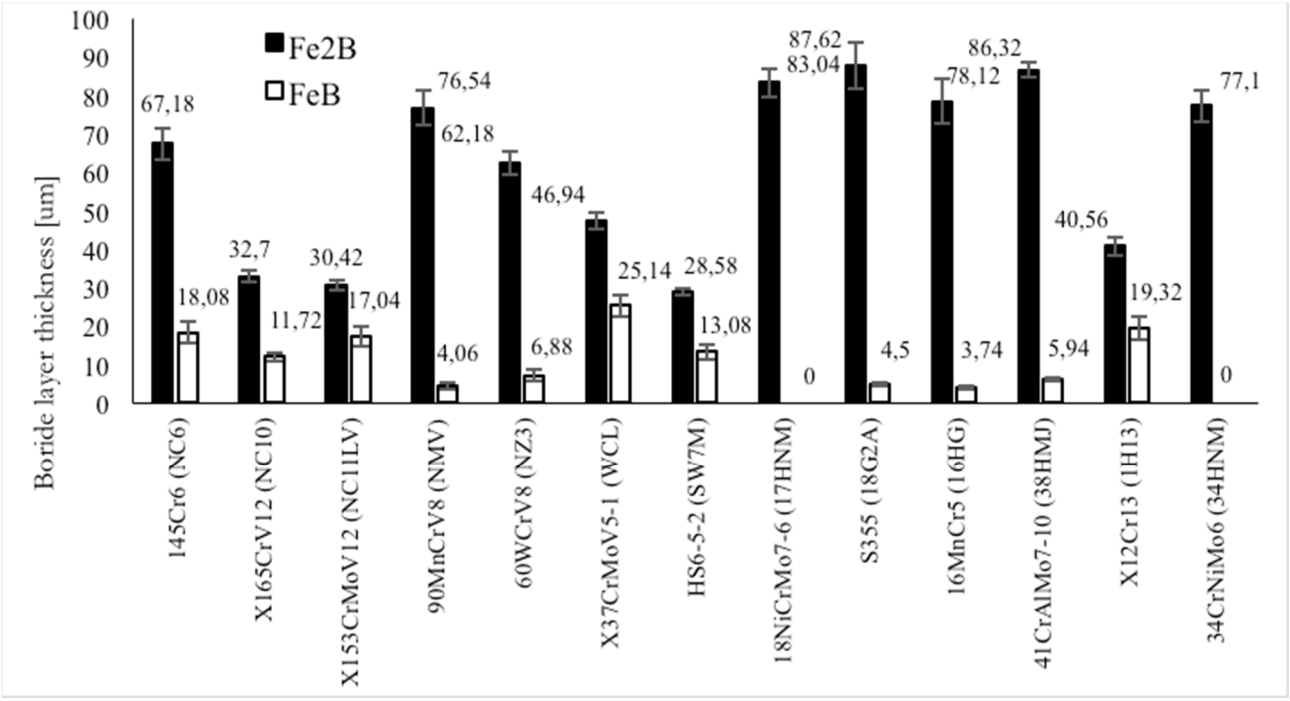


***Fig. 14*** *Average thickness of boride layers produced using EKABOR-2 powder on the steel grades tested*

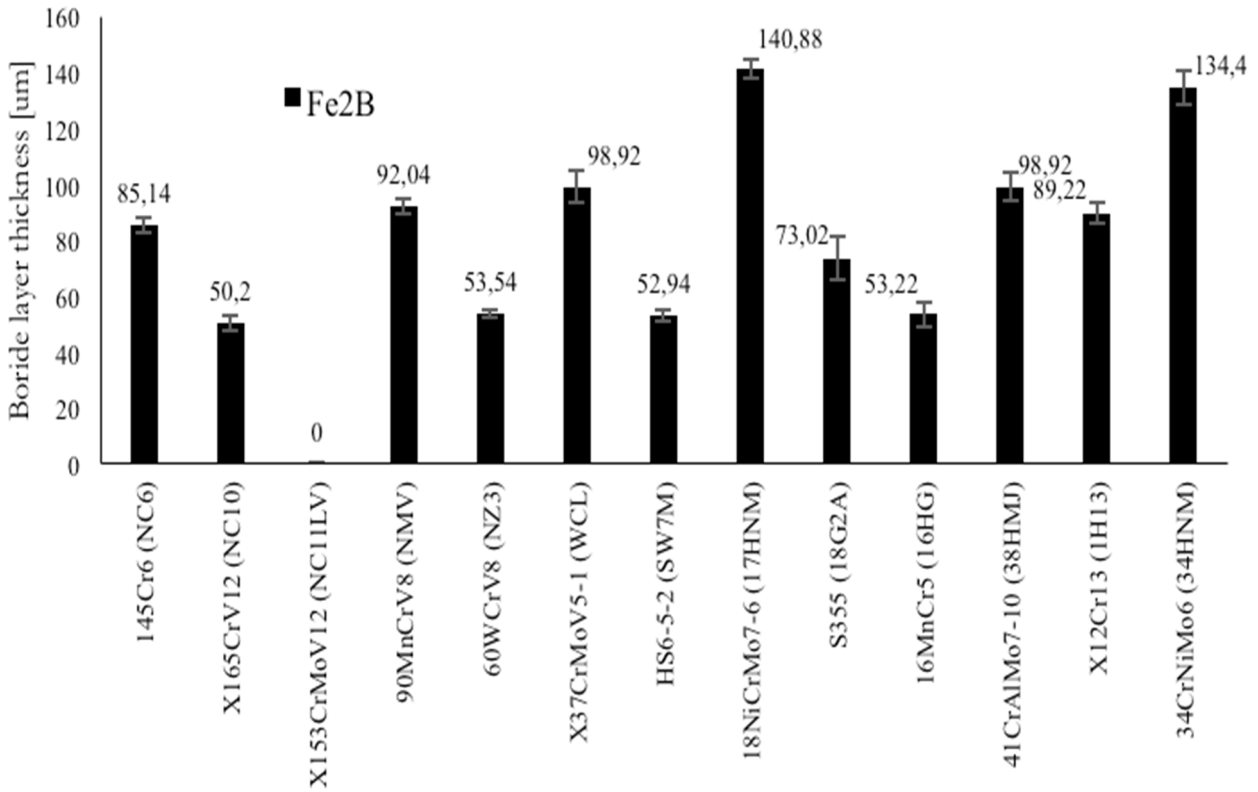


***Fig. 15*** *Average thickness of boride layers produced with EKABOR-PASTE paste on the steel grades tested*

***Tab. 2*** *Classification of the obtained boride layers produced on the substrates of the investigated steel grades using EKABOR-2 powder and EKABOR-PASTE paste (1000°C/4h) according to Voroshnin and Lyakhovich (NC- discontinuous boride layer, C-continuous boride layer) [19].*

| Classification according to Voroshnin and Lyakhovich [19] | | | | |
|---|---|---|---|---|
| Steel grade | EKABOR-2 | | EKABOR-PASTE | |
| | Structure model | Structure components | Structure model | Structure components |
| 145Cr6 (NC6) | I | FeB (C) + $Fe_2B$ (C) | II | Fe2B (C) |
| X165CrV12 (NC10) | I | FeB (C) + $Fe_2B$ (C) | II | Fe2B (C) |
| X153CrMoV12 (NC11LV) | I | FeB (C) + $Fe_2B$ (C) | - | - |
| 90MnCrV8 (NMV) | XI | FeB (NC) + $Fe_2B$ (C) | II | Fe2B (C) |
| 60WCrV8 (NZ3) | II | $Fe_2B$ (C) | IX | Fe2B (NC) |
| X37CrMoV5-1 (WCL) | I | FeB (C) + $Fe_2B$ (C) | II | Fe2B (C) |
| HS6-5-2 (SW7M) | IV | Fe(B) | IV | Fe(B) |
| 18NiCrMo7-6 (17HNM) | II | $Fe_2B$ (C) | II | Fe2B (C) |
| S355 (18G2A) | XI | FeB (NC) + $Fe_2B$ (C) | IX | Fe2B (NC) |
| 16MnCr5 (16HG) | II | $Fe_2B$ (C) | IX | Fe2B (NC) |
| 41CrAlMo7-10 (38HMJ) | XI | FeB (NC) + $Fe_2B$ (C) | IX | Fe2B (NC) |
| X12Cr13 (1H13) | I | FeB (C) + $Fe_2B$ (C) | II | Fe2B (C) |
| 34CrNiMo6 (34HNM) | II | $Fe_2B$ (C) | II | Fe2B (C) |

## 5 Conclusions

- The type of boriding medium (pack, paste) and the content of alloying elements in the steel affect the thickness and morphology of the boride layers.
- A high content of alloying elements increasing the content of the FeB phase (Cr, Mo, W), results in an outer continuous layer of FeB borides.
- As the content of alloying elements and carbon increases, the total thickness of the boride coatings decreases.
- Chromium content below about 1%, with carbon content below about 0.4%, significantly limits or prevents the formation of FeB phase.
- Increasing content of alloying elements and carbon, results in a change in boride morphology according to the scheme: thin, sharply pointed needles thick, bluntly pointed needles branched needles flat boride/steel substrate interfacial boundary.
- Higher porosity was observed in the near-surface zone of boride coatings produced using EKABOR-PASTE paste.
- Further studies are required to further investigate the boride coatings formed and to determine their chemical and phase composition.

## Acknowledgement

***The research was financially supported by National Research and Development Centre under grant no. TECHMATSTRATEG-III/0002/2019***

## References

[1] MOISSAN, H. (1895). CR hebdom Seances Acad. Sci 120, 74

[2] BARTKOWSKA, A.; PERTEK-OWSIANNA, A.; BARTKOWSKI, D. (2015). Odpornosc korozyjna stali C45 po borowaniu dyfuzyjnym i laserowym. *Inzynieria Materialowa 2* (204), 78-81

[3] KAOUKA, A.; ALLAF, H.; KEDDAM, M.; ALAOUI, O. (2022). Evaluating the Corrosion Behaviour of Borided Carbon Steel C35. *Materislas Research 25*, 1-8

[4] GUNES, I.; ERDOGAN, M.; CELIK, A. G. (2014). Corrosion Behaviour and Characterisation of Plasma Nitrided and Borided AISI M2 Steel. *Materials Research 17* (3), 612-618

[5] SU, Z. G.; TIAN, X.; AN, J.; LU, Y.; YANG, Y. L.; SUN, S. J. (2009). Investigation on Boronizing of N80 Tube Steel. *ISIJ International 49* (11), 1776-1783

[6] NORA, R.; ZINE, T. M.; ABDELKADER, K.; YOUCEF, K.; ALI, O.; JIANG, X. (2019). Boriding and boronitrocarburising effects on hardness,wear and corrosion behawior of AISI 4130 steel. *Revista Materia 24* (1),

[7] KAOUKA, A.; ALAOUI, O. (2019). Characterization and corrosion resistance of boride layers on carbon steel. *Materials Science and Engineering 477*,

[8] ERDOGAN, M.; GUNES, I. (2013). Corrosion Behaviour and Microstructure of Borided Tool Steel. *Revista Materia 20* (2), 523-529

[9] KHENIFER, M.; ALLAOUI, O.; TAOUTI, M. B. (2017). Effect of Boronizing on the Oxidation resistance of 316L Stainless Steel. *Acta Physica Polonica 132* (3), 518 - 520

[10] SIEPAK, J. (1988). Dyfuzyjne borowanie stali w proszkach. Rocznik Naukowo – Dydaktyczny. *Prace Techniczne 4*, 79 – 100

[11] CAMPOS-SILVA, I. E.; RODRIGUEZ-CASTRO, G. A. (2015). Thermochemical Surface Engineering of Steels. Boriding to improve the mechanical properties and corrosion resistance of steels. *Cambridge: Woodhead Publishing*

[12] YORULMAZ, M. A. (2007). An investigation of boriding of medium carbon steels. Marmara University, Faculty of Engineering

[13] GUNEN, A.; KANCA, E. (2017). Microstructure and Mechanical Properties of Borided Inconel 625 Superalloy. *Revista Materia 22* (2),

[14] DZIARSKI, P.; KULKA, M.; MAKUCH, N.; MIKOŁAJCZAK, D. (2017). Corrosion resistance of laser-borided Inconel 600 alloy. *Inzynieria Materialowa 3* (217), 149 - 156

[15] YAO, Q.; SUN, J.; FU, Y.; TONG, W.; ZHANG, H. (2016). An Evaluation of a Borided Layer Formed on Ti-6Al-4V Alloy by Means of SMAT and Low-Temperature Boriding. *Materials 6*, 993 – 1003

[16] KAOUKA, A.; BENAROUS, K. (2020). Characterization and Properties of Boriding Titanium Alloy Ti6Al4V. *Acta Physica Polonica 137* (4), 493 – 495

[17] ZOUZOU, C.; KEDDAM, M.; BOUAROUR, B.; PIASECKI, A.; MIKLASZEWSKI, A.; KULKA, M. (2020). Characterisation of boronizing kinetics of EN-GJL-250 lamellar gray cast iron. *Annales de Chimie – Science des Materiaux 44* (1), 23 - 38

[18] KULKA, M. (2019). Current Trends in Boroding: Techniques. *Cham: Springer Nature Switzerland*

[19] PRZYBYLOWICZ, K. (2000). Teoria i praktyka borowania stali. *Kielce: Wydawnictwo Politechniki Swietokszyskiej*

[20] OZBEK, I.; BINDAL, C. (2011). Kinetics of borided AISI M2 high speed steel. *Vacuum 86*, 391-397

[21] IPEK, M.; EFE, G. C.; OZBEK, I.; ZEYTIN, S.; BINDAL, C. (2012). Investigation of Boronizing Kinetics of AISI 51100 Steel. *Journal of Materials Engineering and Performance 21* (5), 733-738

[22] KAYALI, Y.; GÜNES, I.; ULU, S. (2012). Diffusion kinetics of borided AISI 52100 and AISI 440C steels. *Vacuum 86*, 1428-1434

[23] AZOUANI, O.; KEDDAM, M.; BRAHIMI, A.; SEHISSEH, A. (2015). Diffusion kinetics of boron in the X200CrMoV12 high-alloy steel. *Journal of Mining and Mettalurgy 51* (1), 49-54

[24] GUNES, I.; OZCATAL, M. (2015). Diffusion kinetics and characterisation of borided AISI H10 steel. *Materials and Technology 49* (5), 759-763

[25] KEDDAM, M.; ABDELLAH, Z. N.; KULKA, M.; CHEGROUNE, R. (2015). Determination of the Diffusion Coeficients of Boron in the FeB and Fe2B Layers Formed on AISI D2 Steel. *Acta Physica Polonica 128* (4), 740-745

[26] DONU-RUIZ, M. A.; HUITRON, D. S.; GARCIA-BUSTOS, E. D.; CORTES-SUAREZ, V. J.; PERRUSQUIA, N. L. (2021). Effect of the Boron Powder on Surface AISI W2 Steel: Experiments and Modelling. *Advances in Materials Science and Engineering* 1-9

[27] CAMPOS-SILVA, I.; ORTIZ-DOMI´NGUEZ, M.; TAPIA-QUINTERO, C.; RODRI´GUEZ-CASTRO, G.; JIME´NEZ-REYES, M. Y.; CHA´ VEZ-GUTIE´RREZ, E. (2012). Kinetics and Boron Diffusion in the FeB/Fe2B Layers Formed at the Surface of Borided High-Alloy Steel. *Journal of Materials Engineering and Performance 21* (8), 1714-1723

[28] DELAI, O.; XIA, C.; SHIQIANG, L. (2021). Growth kinetics of the FeB/Fe2B boride layer on the surface of 4Cr5MoSiV1 steel: experiments and modeling. *Journal of Materials Research and Technology 11*, 1272-1280

[29] ABDELLAH, Z. N.; KEDDAM, M.; ELIAS, A. (2012). Modelling the Boronizing Kinetics in AISI 316 Stainless Steel. *Acta Phisica Polonica 122* (3), 588-592

[30] MEBAREK, B.; KEDDAM, M. (2019). Prediction Model for Studying the Growth Kinetics of Fe2B Boride Layers during Boronizing. *Ingénierie des Systèmes d'Information 24* (2), 201-205

[31] LITORIA, A. K.; FIGUEROA, C. V.; BIM, L. T.; PRUNCU, C. I.; JOSHI, A. A.; HOSMANI, S. S. (2019). Pack-boriding of low alloy steel: microstructure evolution and migration behaviour of alloying elements. *Philosophical Magazine* 1-26

[32] HERNANDEZ-SANCHEZ, E. ET AL. (2014). A Study on the Effect of the Boron Potential on the Mechanical Properties of the Borided Layers Obtained by Boron Diffusion at the Surface of AISI 316L Steel. *Hindawi Publishing Corporation* 1-9

[33] ALLAOUI, O.; BOUAOUADJA, N; SAINDERNAN, G. (2006). Characterization of boronized layers on a XC38 steel. *Surface and Coatings Technology* 201, 3475-3482

[34] GUNES, I.; YILDIZ, I. (2016). Investigation of Adhesion and Tribological Behavior of Borided AISI 310 Stainless Steel. *Revista Materia 21* (1), 61-71

[35] HAYAT, F.; SEZGIN, C. T. (2021). Wear Behavior of Borided Cold-Rolled High Manganese Steel. *Coatings 11* (1207), 1-21

[36] MUHAMMAD, W. (2013). Boriding of high carbon high chromium cold work tool steel. *Materials Science and Engineering* 60, 1-6

[37] GARCIA-LEON, R. A.; MARTINEZ-TRINIDAD, J.; CAMPOS-SILVA, I.; WONG-ANGEL, W. (2019). Mechanical characterization of the AISI 316L alloy exposed to boriding proces. *DYNA* 87 (213), 34-41

[38] HERNANDEZ-SANCHEZ, E. ET AL. (2019). Tribological Behaviour of Borided AISI 316L Steel with Reduced Friction Coefficient and Enhanced Wear Resistance. *Materials Transactions* 60 (1), 156-164

[39] CARDENAS, V. E. ET AL. (2016). Characterization and wear performance of boride phases over tool steel substrates. *Advances in Mechanical Engineering* 8 (2), 1-10

[40] GUNES, I.; OZCATAL, M. (2016). Investigation of the adhesion and wear properties of borided AISI H10 steel. *Materials and Technology* 50 (2), 269-274

[41] GUNES, I.; KANAT, S. (2016). Investigation of wear behaviour of borided AISI D6 steel. *Materials and Technology* 50 (4), 505-510

[42] AKTAS, B.; TOPRAK, M.; ÇALIK, A.; TEKGÜLER, A. (2020). Effect of pack-boriding on the tribological behavior of Hardox 450 and HiTuf Steels. *Reviewse on Advanced Materials Science* 59, 314-321

[43] KAOUKA, A.; ALLAOUI, O.; KEDDAM, M.; TAKTAK. (2013). Properties of borided SAE 1035 steels and fracture toughness produced by Vickers indentation. *Surface Effects and Contact Mechanics* 78, 183-191

[44] TÜRKMEN,.; YALAMAÇ, E. (2018). Growth of the $Fe_2B$ layer on SAE 1020 steel employed a boron source of H3BO3 during the powder-pack boriding method. *Journal of Alloys and Compounds*, doi: 10.1016/j.jallcom.2018.02.118

[45] OLIVEIRA, C. K. N.; CASTELETTI, L. C.; LOMBARDI LETO, A.; TOTTEN, G. E.; HECK, S. C. (2010). Production and characterisation of boride layers on AISI D2 steel. *Vacuum* 84, 792-796

[46] ATIK, E.; YUNKER, U.; MERIC, C. (2003). The effects of conventional heat treatment and boronizing on abrasive wear and corrosion of SAE 1010, SAE 1040, D2 and 304 steels. *Tribology International* 36, 155-161

[47] BALUSAMY, T.; SANKARA NARAYANAN, T. S. N.; RAVICHANDRAN, K.; SONG PARK, I.; LEE, M. H. (2013). Pack boronizing of AISI H11 tool steel: Role of surface mechanical attrition treatment. *Vacuum* 97, 36-43

[48] BOUMAALI, B.; ABDELLAH, N. Z.; KEDDAM, M. (2021). Characterisation of bilayer (FeB/Fe2B) on AISI H13 work tool steel. *Koroze a ochrana materiálu* 65 (2), 40-48

[49] DONU RUIZ, M. A. ET AL. (2015). Growth kinetics of boride coatings formed at the surface AISI M2 during dehydrated paste pack boriding. *Thin Solid Films* 596, 147-154

[50] CALIK, A.; UCAR, N.; KOCASLAN, A.; KARAKAS, S. (2017). Effect of interrupted boriding on microstructure and mechanical

properties of 16MnCr5 steels. *Surface Review and Letters* 1950022, 1-6

[51] ANGKURARACH, L.; JUIJERM, P. (2012). Effects of direct current field on powder-packed boriding proces on martensitic stainless steel AISI 420. *Archieves of Metallurgy and Materials* 57 (3), 799-804

[52] GUNES, I. (2014). Investigation of Tribological Properties and Characterization of Borided AISI 420 and AISI 5120 Steels. *Transactions of the Indian Institute of Metals* 67 (3), 359-365

[53] UCAR, N.; YIGIT, M.; CALIK, A. (2020). Metallurgical characterisation of borided 34CrNiMo6 steel. *Advances in Materials Science* 20 (4), 38-48

[54] UCAR, N.; YIGIT, M.; CALIK, A. (2020). Boriding of 34CrNiMo6 Steels. *Chemistry Research Journal* 5 (2), 71-74

[55] DYCHTON, K., KOCUREK, P., ROKICKI, P., WIERZBA B., DRAJEWICZ, M., SIENIAWSKI, J., Microstructure and residual stress in AMS 6308 steel after vacuum carburizing and gas quenching, *Acta Physica Polonica A*, 2016, 130(4), pp. 953–955

[56] NOVÁ I., MACHUTA J., Monitoring of the Diffusion Processes during Carburizing Automotive Steel Parts, *Manufacturing Technology*, 2016, 16(1): pp. 225-230, DOI: 10.21062/ujep/x.2016/a/1213-2489/MT/16/1/225

[57] FALTEJSEK P., JOSKA Z., POKORNÝ Z., DOBROCKÝ D., STUDENÝ Z., Effect of Nitriding on the Microstructure and Mechanical Properties of Stainless Steels, *Manufacturing Technology* 2019, 19(5):745-748 | DOI: 10.21062/ujep/365.2019/a/1213-2489/MT/19/5/745

[58] DRAJEWICZ, M., GÓRAL, M., KOSCIELNIAK, B., OCHAL K., KUBASZEK T., PYTEL M., WIERZBA, P., WOJTYNEK, R., The influence of process parameters on structure and phase composition of boride coatings obtained on x39crmo17-1 stainless steel, *Solid State Phenomena*, 2021, 320 SSP, pp. 55–59

[59] BRICÍN D., KŘÍŽ A., NOVOTNÝ J., ŠPIRIT Z., The Effect of Boriding And Heat Treatment on the Structure and Properties of 100Cr6 Steel, *Manufacturing Technology* 2022, 22 (1): pp.2-9, DOI: 10.21062/mft.2022.003

[60] BRICÍN D., KŘÍŽ A., Influence of the Boriding Process on the Properties and the Structure of the Steel S265 and the Steel X6CrNiTi18-10, *Manufacturing Technology* 2021, 21(1): pp. 37-44 DOI: 10.21062/mft.2021.003

[61] DRAJEWICZ, M., GÓRAL, M., PYTEL, M., KOSCIELNIAK B., KUBASZEK T., .WIERZBA P., CICHOSZ P., The duplex coating formation using plasma nitriding and crn pvd deposition on x39crmo17-1 stainless steel, *Solid State Phenomena*, 2021, 320 SSP, pp. 43–48